



UvA-DARE (Digital Academic Repository)

Nanocatalysts: Properties and applications

Gaikwad, A.V.

Publication date
2009

[Link to publication](#)

Citation for published version (APA):

Gaikwad, A. V. (2009). *Nanocatalysts: Properties and applications*. [Thesis, fully internal, Universiteit van Amsterdam].

General rights

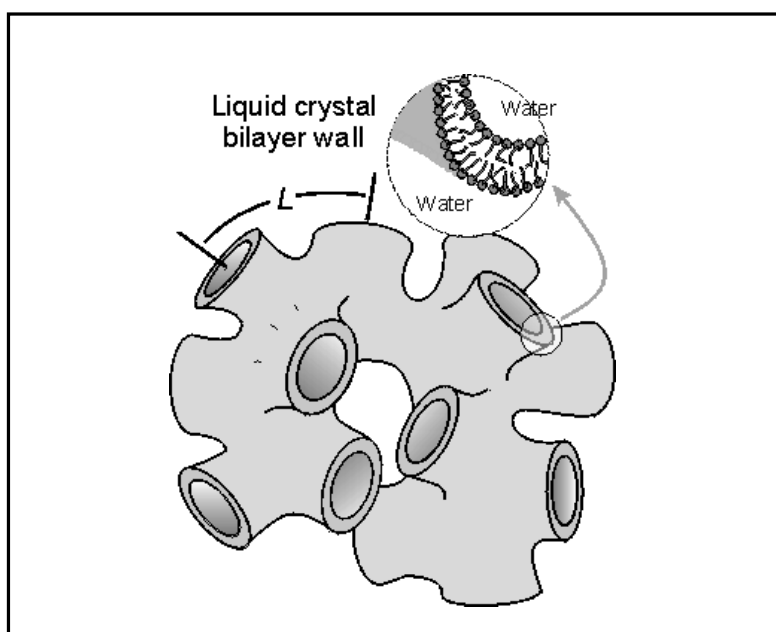
It is not permitted to download or to forward/distribute the text or part of it without the consent of the author(s) and/or copyright holder(s), other than for strictly personal, individual use, unless the work is under an open content license (like Creative Commons).

Disclaimer/Complaints regulations

If you believe that digital publication of certain material infringes any of your rights or (privacy) interests, please let the Library know, stating your reasons. In case of a legitimate complaint, the Library will make the material inaccessible and/or remove it from the website. Please Ask the Library: <https://uba.uva.nl/en/contact>, or a letter to: Library of the University of Amsterdam, Secretariat, Singel 425, 1012 WP Amsterdam, The Netherlands. You will be contacted as soon as possible.

Chapter 4

Stable ‘soap and water’ sponges doped with metal nanoparticles



Part of this work is submitted to a journal as “Stable soap and water sponges doped with metal nanoparticles”, A. V. Gaikwad, P. G. Verschuren, T. van der Loop, G. Rothenberg, and E. Eiser.

Introduction

Surfactant-cosurfactant molecules in solution can self-organize into various assemblies including lamellae, hexagonal or cubical crystals, and vesicles.^[1-4] One particularly fascinating phenomenon is the formation of “supramolecular sponges”, technically known as bicontinuous L_3 phases.^[5] Our first understanding of these strange structures comes from the pioneering works of Porte^[6] and Cates.^[7] The L_3 phase is a bilayer membrane with a randomly connected interphase separating two interpenetrating labyrinths of solvent (see Figure 1). L_3 phases are typically transparent, and flow easily (in contrast to the highly viscous L_α lamellar phases).^[8, 9] They have been observed and studied in various surfactant and polymer solutions,^[10-14] as well as using computer simulations.^[7, 15]

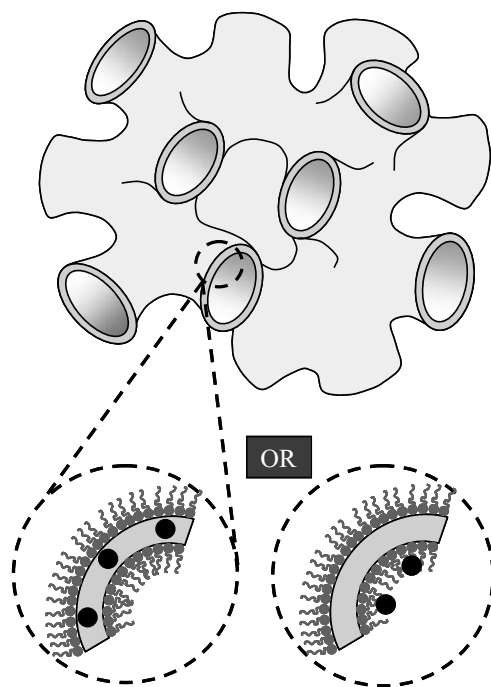


Figure 1. Schematic image of pure and doped sponge phase.

Recently, the L_3 sponge phases have attracted much attention in materials science,^[16-19] as templates for making novel porous materials.^[20] The applications include filtration,^[21, 22] biological separation,^[23] drug delivery,^[24] and making new catalysts and supports.^[16, 25-27] The main problem, however, is that L_3 phases are typically unstable, especially over varied temperature ranges. Our experience with trapping metal

nanoparticles in hexagonal soft crystal gels,^[1, 28] has led us to the idea of stabilising L₃ phases by doping them with metal nanoparticles.^[29] Indeed, such stabilisation was observed also for lamellar phases.^[30-35]

In this paper, we study the stability of sponge phases doped with various metal nanoparticles. To the best of our knowledge, this is the first report of such doped L₃ phases. The nanoparticles, organosols as well as aquasols, are prepared and integrated into the sponge phase. The role of shear-induced structural transitions and the effect of temperature on this doped sponge phase is also reported and discussed.

Experimental section

Materials and Instrumentation. High-energy small-angle X-ray scattering (SAXS) and wide angle X-ray scattering (WAXS) measurements were performed at the BM26 High Brilliance Dutch-Belgium beam line (DUBBLE) at the European Synchrotron Radiation Facility (ESRF) in Grenoble. The sample-to-detector distance was fixed at 3.5 m. The energy of the X-ray photons was 18 keV ($\lambda = 1.54 \text{ \AA}$, exposure time 3 min). A differential scattering calorimetry cell (Linkam optical DSC600) was used, allowing simultaneous X-ray scattering and temperature measurements. Cross-polarized optical microscopy was performed using an Olympus BH-2 microscope coupled to a Leica DM-IRB digital camera. Centrifuging was performed using an Eppendorf 5412 centrifuge at 200 g. UV-visible measurements were performed using a Carry-50 spectrophotometer (quartz cuvette, Hellma Benelux, approximately 3.5 mL, path length 1 cm). The recorded wavelength range was 190–1100 nm, at 1 nm resolution. Rheometric measurements were made using a Haake RS150 instrument. Unless noted otherwise, chemicals were purchased from commercial sources (>99% pure) and used as received. All aqueous solutions were made with Millipore water. Nanoparticles in aqueous and organic solvents were prepared following published procedures.^[41, 47, 48]

Preparation of sponge phase samples. *Example: 70% cyclohexane.* SDS/H₂O solution (20 ml, 1:2.5 weight ratio) was prepared by adding SDS (8 g, 0.02 mole) to water (12 ml). 0.69 ml of this solution was thoroughly mixed with 0.21 ml of pentanol. Then, 2.1 ml of cyclohexane was slowly added while stirring. The sample was sealed and stored in an oven at 25 °C. Other sponge phase samples were similarly prepared using the reagent quantities given in Table 1.

Procedure for doping the sponge phase with metal nanoparticles. Au aquasols were prepared using the method described by Turkevich *et al.*⁴¹ A stock solution of

HAuCl₄ (20 ml, 1 mM) was prepared in water and mixed with a sodium citrate solution (2 ml, 34 mM). The mixture was vigorously stirred and heated at 100 °C for 5 min. The resulting red suspension was concentrated to *ca.* 2 ml by centrifuging. 120 µl of the suspension was added to a 3.0 ml sponge phase sample, prepared as above, and stirred for 30 min at 25 °C. The color of the sponge phase changed from colorless to a transparent pink. Sponge phase samples containing Pd and Ag aquasols were analogously prepared.

Au organosols were prepared using a modification of the method described by Yee *et al.*^[48] Here, 165 mg (0.82 mmol) of dodecanethiol was added under vigorous stirring to a solution of 1.0 mmol HAuCl₄ in 10 mL of freshly distilled, anhydrous THF. 1.00 ml of 1.0 M solution of lithium triethylborohydride in THF was added dropwise to the reaction mixture until no more gas evolved, and the mixture was then stirred for 20 min at 25 °C. The resulting dark red-brown suspension was washed with 20 ml of ethanol and concentrated to *ca.* 1 ml by centrifuging. 120 µl of this concentrated suspension was added to a 3 ml sponge phase sample and stirred for 30 min at 25 °C. Samples were analyzed by cross-polarized microscopy, confirming the isotropic structure.

Results and Discussion

The sponge phases were prepared using a sodium dodecyl sulfate solution (SDS:H₂O, 1:2.5 w/w ratio), pentanol as co-surfactant and cyclohexane as the oil phase. We prepared four samples with different cyclohexane amounts (Table 1)^[36] and vigorous stirring for 30 min yielded the transparent sponge phase, which was stable at 25–30 °C. The pentanol:(SDS/H₂O) weight ratio was 0.9–1.2. Note that stirring is critical – improper mixing results in an ordered phase, especially at lower cyclohexane concentrations. The L₃ phase exists only in a very narrow range of the oil-rich corner in the phase diagram (>70% cyclohexane). The pores of this phase contain cyclohexane, while the membrane contains water. Cross-polarized optical microscopy confirmed that the samples were optically isotropic. Samples with < 65% cyclohexane showed birefringence, *i.e.* formation of a lamellar phase (Table 1, entry 4).^[37]

Table 1. Composition of L₃ phase and their properties.

Entry	SDS/H ₂ O ^a %	Pentanol % ^a	Cyclohexane % ^a	D ^b (nm)	δ ^c (nm)
1	23.0	6.9	70.1	31.4	3.6
2	18.7	6.4	74.9	35.0	3.5
3	14.8	6.4	79.1	40.8	3.0
4 ^d	28.7	7.6	63.7	27.3	3.9

^a The component fractions are given in terms of vol% at 25 °C. ^b D is the characteristic distance corresponding to the cell size calculated directly from the q_{\max} values of the SAXS profiles. ^c δ is the membrane thickness. ^d This sample did not yield a sponge phase.

Figure 2 shows the SAXS spectra of the three sponge phases prepared using different amounts of cyclohexane at 25 °C (Table 1, entries 1–3). At higher cyclohexane concentrations, the intensity peaks move to lower length scales. Bilayer structures such as L_α and L₃ phases are known to follow a q^{-2} dependence.^[38-40] In all three samples, the peak intensity showed a similar dependence ($q^{-2.3}$, $q^{-2.4}$, and $q^{-2.6}$ for 70%, 75%, and 80% cyclohexane, respectively). This dependence, combined with the broadness of the peaks, confirms the formation of the L₃ sponge phase. Above 30 °C, all samples underwent a phase change to an L_α phase, showing sharp second- and third-order peaks. Porte *et al.* demonstrated that the length scale at maximum intensity value (q_{\max}) correlates with the characteristic distance (D), or cell size in the case of sponge phase, according to

$$D = \frac{2\pi}{q_c} = \alpha \frac{\delta}{\phi_w} \quad (1)$$

where ϕ_w is the sheet volume fraction here as equal to the water volume fraction.^[5] The connectivity parameter α is roughly 1.5 for smooth bicontinuous structures.^[38] Table 1 lists the corresponding D and δ values. Note that at higher cyclohexane concentrations, the sponge phase swells, increasing the cell size and decreasing the membrane thickness.

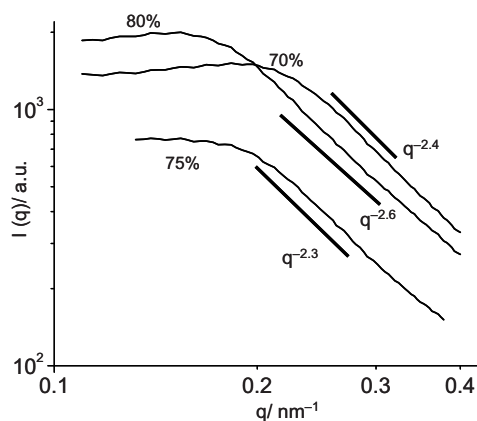


Figure 2. Logarithmic SAXS spectra of sponge phases prepared using different amounts of cyclohexane at 25 °C.

Once we confirmed the sponge-like structure of our samples, we doped them with small amounts of different metal nanoparticles. Aquasols of gold, palladium, and silver nanoparticles were prepared following published protocols,^[41] and analyzed using UV-visible spectroscopy.^[42] The particle diameters were 8–10 nm, calculated using the surface plasmon peak correlation method.^[42, 43] The colloidal suspensions were concentrated by centrifuging, and 4% v/v of the concentrated suspension was added to each sponge phase sample. The samples were then sealed and stirred at 25 °C for 30 min, giving a clear liquid that showed no birefringence under cross-polarized microscopy.

Figure 3 shows the SAXS spectra of sponge phase samples doped with gold nanoparticle aquasols. The inset shows the Bragg rings of crystalline gold in these samples. Optical microscopy showed no aggregation, confirming that the particles are well dispersed. Additional wide angle X-ray scattering (WAXS) measurements confirmed the presence of Au particles inside the samples. The nanoparticles cause the membrane to swell, increasing q_{max} . The swelled regions of the membranes showed average δ values of 13–15 nm.

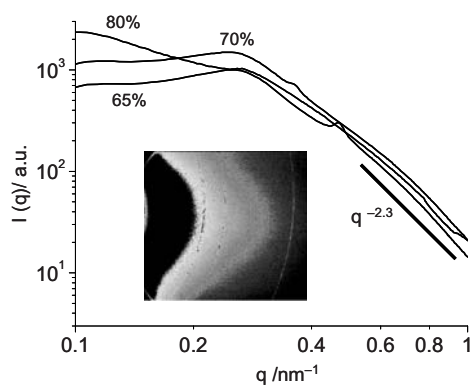


Figure 3. Logarithmic SAXS spectra of the sponge phase samples doped with 4% v/v of a gold nanoparticle suspension. The inset shows the WAXS image of the Au-doped sample made with 70% cyclohexane (image taken at 5 min exposure time).

These doped sponge phases also display interesting optical properties. The original gold cluster suspension is pink, but the doped phase is violet in reflection and blue in transmission. This change was confirmed with UV-visible spectroscopy measurements (Figure 4). Aqueous suspensions of gold nanoparticles show a typical plasmon absorption peak at $\lambda = 520$ nm. Conversely, when the particles were dispersed in the sponge phase, we observed two peaks at $\lambda = 511$ and $\lambda = 700$ nm. Indeed, gold nanoparticles are known to have different plasmon peaks depending on their alignment and relative positioning.^[43] These two peaks may indicate that the nanoparticles that are confined in the membrane align along two different pore directions. Extending the scope of this approach to other metals, we prepared Pd-doped and Ag-doped sponge phases, as well as an Au-doped phase using thiol-stabilized gold organosols (Figure 5). In all cases, the metal particle diameters were much smaller than the gold aquasols above, *ca.* 2–3 nm. All samples were stable at 25 °C.

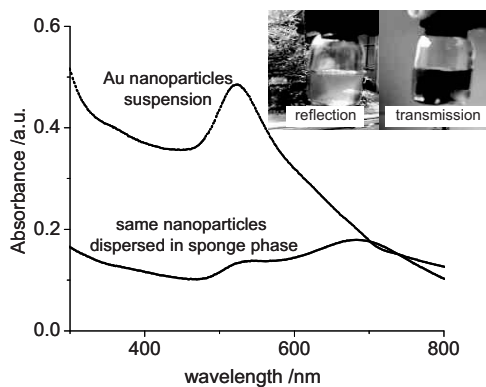


Figure 4. UV-Visible spectra of an aqueous gold nanoparticle suspension and the same suspension doped in a sponge phase prepared with 70% v/v cyclohexane. The inset shows the color changes under reflection and transmission conditions.

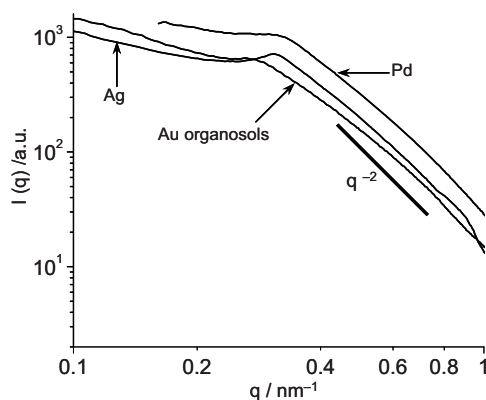


Figure 5. Logarithmic SAXS spectra of sponge phase samples (70% v/v cyclohexane), doped with 4% v/v of metal nanoparticle suspension.

Having shown the possibility of doping sponge phases with different metal clusters, we now focused on studying their stability, a key parameter in many practical applications. We carried out rheometric studies for different samples, using a cylindrical container and constant shear rates. Figure 6 shows the viscosity/shear dependence for the pure (*i.e.*, “empty”) sponge phase, as well as for the gold-doped sample. To obtain steady-state viscosities, every measuring point was taken after 30 s at a constant shear stress (note that the relaxing time was determined only at the lowest shear stress). The increasing shear

stress measurements for both samples showed a Newtonian behaviour (part I) and a shear thinning behaviour (part II), with the transition at around 100 s^{-1} shear rate. This also agrees with the optical measurements of Porcar *et al.*,^[44] who attributed the first part to a sponge phase and the second part to a lamellar phase.

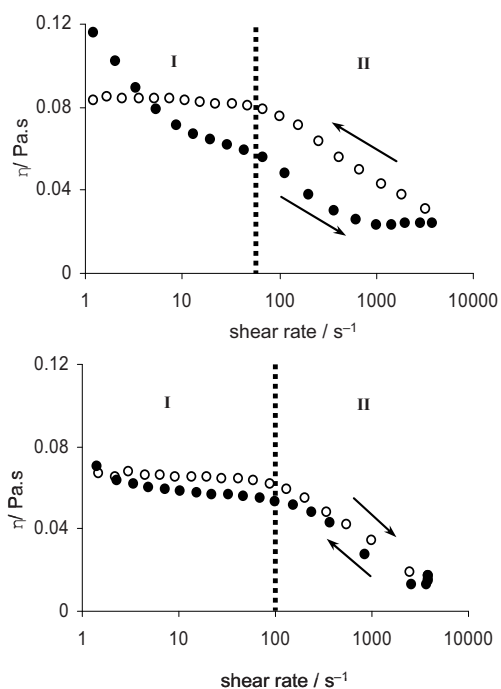


Figure 6. Semi-logarithmic plot of viscosity *vs.* shear rate of a pure sponge phase sample (top), and the same sample doped with 4% v/v gold nanoparticles suspension (bottom). ‘o’ symbols denote measurements at increasing shear rates, while ‘●’ symbols pertain to measurements at decreasing shear rates. In both cases, the transition between the sponge phase I and the lamellar phase II occurs at around 100 s^{-1} shear rate.

Decreasing the shear stress back for the “empty” sample did not regenerate the sponge phase, in agreement with the observations of Mahjoub^[45] and Porcar.^[46] The latter suggested that this irreversible transformation was due to pentanol evaporation. Surprisingly, the gold-doped sample *did* revert to its original sponge structure when the shear stress was decreased. We suggest that this reversibility stems from the increased stability of the doped sponge phase. The presence of nanoparticles increases the

membrane's bending rigidity. Note that a similar behaviour was also observed for doped lamellae.^[31,33]

We also examined the temperature stability of gold-doped sponge phase samples (Figure 7). At 25 °C, we obtained using SAXS the typical broad spectrum of the sponge phase. At 40 °C, an additional sharp ring appeared, and at 60 °C a sharp ring was observed (see inset photo). The sharp ring points to a lamellar phase. Re-cooling the sample down to 40 °C, we observed again the broad peak, together with a less pronounced ring. This shows that the transformation is indeed reversible. Additional WAXS measurements also confirmed that the gold particles are crystalline, and that even at 60 °C the particles are still intact in the membrane.

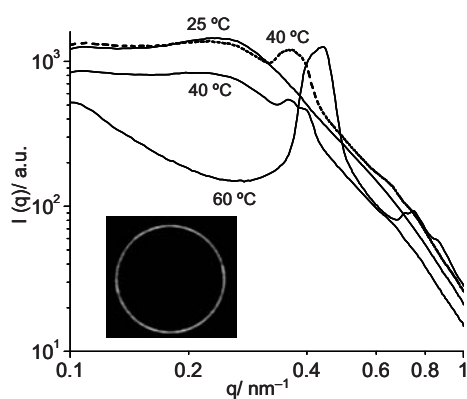


Figure 7. Logarithmic SAXS plot of the gold-doped sponge phase sample, prepared using 70% v/v cyclohexane, at different temperatures. The inset photo shows the SAXS image taken at 60 °C.

We then compiled the partial phase diagram of the doped and undoped samples with different amounts of cyclohexane. Figure 8 shows the diagram for the “empty” samples (top) and for samples doped with 4% v/v Pd nanoparticle aquasols suspension (bottom). All these samples were studied with SAXS in a sealed capillary, to avoid any evaporation. The Pd-free samples containing low cyclohexane amounts (60% and 65%) yielded hexagonal phases at lower temperatures, and lamellae at higher temperatures. The sponge phase exists only in a narrow range (between 70–80% cyclohexane), and transforms to a lamellar phase above 40 °C. Conversely, the Pd-doped samples containing

low cyclohexane amounts maintained a hexagonal phase at lower as well as at higher temperatures. Significantly, the sponge phases of Pd-doped samples made with 70–80% cyclohexane were stable upto 50 °C. This clearly shows that doping the sponge phase with a small amount of nanoparticles increases its stability at higher temperatures.

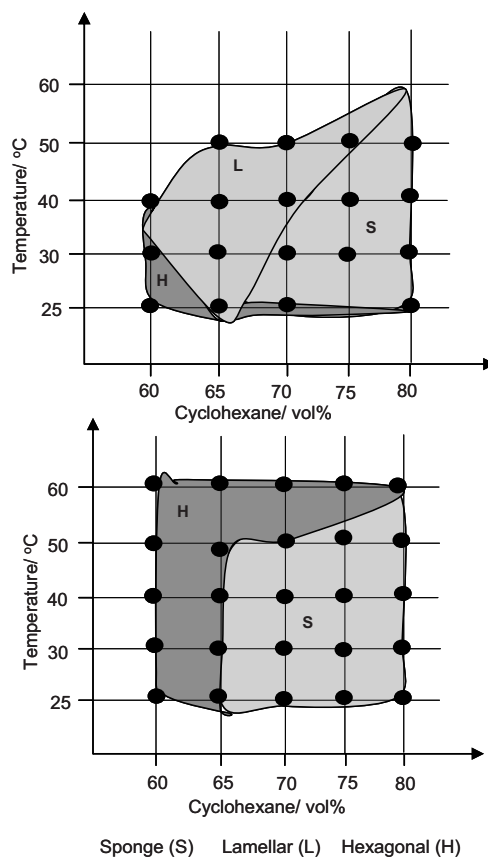


Figure 8. Partial phase diagrams of “empty” (top) and Pd-doped samples (bottom), prepared with different amounts of cyclohexane.

Conclusions.

We showed here that “soap and water” sponge phases are stabilised by the addition of metal nanoparticles. These metal-doped sponges retain their phase composition and structure over a much wider temperature range compared to the undoped, “empty” samples. The stabilisation can be performed both with organosols and aquasols, and using different metals. Furthermore, while the empty sponge phases are irreversibly changed under shear stress, the metal-doped sponge samples show a reversible behaviour,

switching between lamellar L_{α} and sponge L_3 phases. We envisage that simple synthetic protocols presented here will open new avenues for applications in catalysis and materials science. These applications will be the subject of future research in our laboratory.

References

- [1] F. Bouchama, M. B. Thathagar, G. Rothenberg, D. H. Turkenburg, E. Eiser, *Langmuir* **2004**, *20*, 477.
- [2] R. G. Laughlin, *Curr. Opin. Coll. Inter. Sci.* **1996**, *1*, 384.
- [3] K. Fontell, *Coll. Poly. Sci.* **1990**, *268*, 264.
- [4] G. Porte, *Curr. Opin. Coll. Inter. Sci.* **1996**, *1*, 345.
- [5] G. Porte, J. Marignan, P. Bassereau, R. May, *J. Physique II* **1988**, *49*, 511.
- [6] G. Porte, M. Delsanti, I. Billard, M. Skouri, J. Appell, J. Marignan, F. Debeauvais, *J. Physique II* **1991**, *1*, 1101.
- [7] M. E. Cates, D. Roux, D. Andelman, S. T. Milner, S. A. Safran, *Europhys. Lett.* **1988**, *5*, 733.
- [8] G. Porte, J. Appell, P. Bassereau, J. Marignan, M. Skouri, I. Billard, M. Delsanti, *Physica A* **1991**, *176*, 168.
- [9] H. Wennerstrom, J. Daicic, U. Olsson, G. Jerke, P. Schurtenberger, *J. Mol. Liq.* **1997**, *72*, 15.
- [10] E. Freyssingas, F. Nallet, D. Roux, *Langmuir* **1996**, *12*, 6028.
- [11] M. Magalhaes, D. Pusiol, M. E. Ramia, A. M. F. Neto, *J. Chem. Phys.* **1998**, *108*, 3835.
- [12] R. Beck, Y. Abe, T. Terabayashi, H. Hoffmann, *J. Phys. Chem. B* **2002**, *106*, 3335.
- [13] I. Javierre, F. Nallet, A. M. Bellocq, M. Maugey, *J. Phys. Cond. Matter* **2000**, *12*, A295.
- [14] R. Strey, W. Jahn, G. Porte, P. Bassereau, *Langmuir* **1990**, *6*, 1635.
- [15] R. Granek, M. E. Cates, *Phys. Rev. A* **1992**, *46*, 3319.
- [16] K. M. McGrath, D. M. Dabbs, N. Yao, I. A. Aksay, S. M. Gruner, *Science* **1997**, *277*, 552.
- [17] S. H. Bhansali, A. S. Malik, J. M. Jarvis, I. Akartuna, D. M. Dabbs, J. D. Carbeck, I. A. Aksay, *Langmuir* **2006**, *22*, 4060.
- [18] G. J. D. Soler-illia, C. Sanchez, B. Lebeau, J. Patarin, *Chem. Rev.* **2002**, *102*, 4093.
- [19] G. Surendran, M. S. Tokumoto, E. P. dos Santos, H. Remita, L. Ramos, P. J. Kooyman, C. V. Santilli, C. Bourgaux, P. Dieudonne, E. Prouzet, *Chem. Mater.* **2005**, *17*, 1505.
- [20] K. M. McGrath, D. M. Dabbs, N. Yao, K. J. Edler, I. A. Aksay, S. M. Gruner, *Langmuir* **2000**, *16*, 398.
- [21] J. S. Beck, J. C. Vartuli, G. J. Kennedy, C. T. Kresge, W. J. Roth, S. E. Schramm, *Chem. Mater.* **1994**, *6*, 1816.
- [22] X. Feng, G. E. Fryxell, L. Q. Wang, A. Y. Kim, J. Liu, K. M. Kemner, *Science* **1997**, *276*, 923.
- [23] M. E. Davis, *Nature* **1993**, *364*, 391.
- [24] J. H. Chang, C. H. Shim, B. J. Kim, Y. Shin, G. J. Exarhos, K. J. Kim, *Adv. Mater.* **2005**, *17*, 634.
- [25] T. Maschmeyer, *Curr. Opin. Solid State Mater. Sci.* **1998**, *3*, 71.
- [26] J. S. Beck, J. C. Vartuli, W. J. Roth, M. E. Leonowicz, C. T. Kresge, K. D. Schmitt, C. T. W. Chu, D. H. Olson, E. W. Sheppard, S. B. McCullen, J. B. Higgins, J. L. Schlenker, *J. Am. Chem. Soc.* **1992**, *114*, 10834.
- [27] G. S. Attard, J. C. Glyde, C. G. Goltner, *Nature* **1995**, *378*, 366.
- [28] E. Eiser, F. Bouchama, M. B. Thathagar, G. Rothenberg, *ChemPhysChem* **2003**, *4*, 526.
- [29] A sample of soft crystal hexagonal phase doped with Pd nanoparticles prepared in April 2003, is still stable after more than four years, showing no phase separation or particle aggregation.
- [30] L. Ramos, P. Fabre, E. Dubois, *J. Phys. Chem.* **1996**, *100*, 4533.
- [31] V. Ponsinet, P. Fabre, *J. Phys. Chem.* **1996**, *100*, 5035.
- [32] W. Wang, S. Efrima, O. Regev, *J. Phys. Chem. B* **1999**, *103*, 5613.
- [33] V. Ponsinet, P. Fabre, *J. Physique II* **1996**, *6*, 955.
- [34] Y. Kimura, T. Mori, A. Yamamoto, D. Mizuno, *J. Phys. Cond. Matter* **2005**, *17*, S2937.
- [35] I. Grillo, P. Levitz, T. Zemb, *Eur. Phys. J. E* **2001**, *5*, 377.
- [36] M. Magalhaes, A. M. F. Neto, A. C. Tromba, *J. Phys. Chem. B* **2004**, *108*, 15962.

- [37] J. Daicic, U. Olsson, H. Wennerstrom, G. Jerke, P. Schurtenberger, *J. Physique II* **1995**, 5, 199.
- [38] N. Lei, C. R. Safinya, D. Roux, K. S. Liang, *Phys. Rev. E* **1997**, 56, 608.
- [39] N. Lei, X. M. Lei, *Langmuir* **1998**, 14, 2155.
- [40] A. Maldonado, W. Urbach, R. Ober, D. Langevin, *Phys. Rev. E* **1996**, 54, 1774.
- [41] J. Turkevich, J. Hillier, P. C. Stevenson, *Discuss. Faraday Soc.* **1951**, 11, 55.
- [42] J. Wang, H. F. M. Boelens, M. B. Thathagar, G. Rothenberg, *ChemPhysChem* **2004**, 5, 93.
- [43] A. V. Gaikwad, P. Verschuren, E. Eiser, G. Rothenberg, *J. Phys. Chem. B* **2006**, 110, 17437.
- [44] L. Porcar, W. A. Hamilton, P. D. Butler, G. G. Warr, *Langmuir* **2003**, 19, 10779.
- [45] H. F. Mahjoub, C. Bourgaux, P. Sergot, M. Kleman, *Phys. Rev. Lett.* **1998**, 81, 2076.
- [46] L. Porcar, W. A. Hamilton, P. D. Butler, G. G. Warr, *Phys. Rev. Lett.* **2002**, 89, 168301/1.
- [47] M. B. Thathagar, J. Beckers, G. Rothenberg, *J. Am. Chem. Soc.* **2002**, 124, 11858.
- [48] C. K. Yee, R. Jordan, A. Ulman, H. White, A. King, M. Rafailovich, J. Sokolov, *Langmuir*, **1999**, 15, 3486.